21st Australasian Fluid Mechanics Conference
Adelaide, Australia
10-13 December 2018

Numerical study of the effects of velocity ratio on co-flow jet characteristics

M. X. Zhang[1] and R. C. Chin[1]

[1] School of Mechanical Engineering

The University of Adelaide, South Australia 5005, Australia

Abstract

In this study, large eddy simulations (LES) of turbulent co-flow jets are performed, aiming at investigating the effects of jet-to-co-flow velocity ratio on the jet characteristics. A fully developed turbulent pipe flow at Re=10000 is employed at the jet outlet in the present work. It is generated in a straight pipe with a validated adequate length to achieve fully developed stage. For the co-flow jet, simulations with different jet-to-co-flow velocity ratios (V_r =3, 6 and 12) are performed to investigate the decay of centreline velocities and turbulence intensities of the jet. Results show a decreasing trend of the velocity decay rate, together with the increasing trends for the peak value and decay rate of turbulence intensities, when the velocity ratio decreases (i.e. higher co-flow velocity). This study is then extended to investigate the probability distribution of passive particles within the jet. It is acquired at above-mentioned different velocity ratios in the particle-laden co-flow jets. The results show a negative correlation between the velocity ratio and particle concentration. The particles have a more concentrated distribution with the decrease of V_r, which agrees with the variation of turbulence intensities in the present work.

Introduction

Turbulent jets exist in numerous industrial applications like combustion and chemical processes. Previous jet flow researches covered the rate and angle of jet spreading, the Reynolds stresses and the decay of the centreline velocity, which contributed to a good understanding of the flow mechanism of turbulent jets [1-3]. In practice, however, co-flow jets are commonly applied instead of the single jet because of their mixing characteristics. Additionally, in most cases, a dispersed phase is included in the jet fluid as well. For instance, the particle-laden turbulent co-flow jet, which is common in gasifiers and furnaces, consists of solid particles suspended in the central jet that are enveloped by the co-flowing gas fluid. The effects of co-flow and the interaction between particles and fluid, significantly influence the particle distribution and fluid behaviour. The complexity of the jet flow increases as well.

The co-flow jet has drawn attention in previous research [4, 5]. They examined the effects of the variables, like the density ratio, and inner nozzle lip thickness on the mixing characteristics of co-flow jets. However, few of the previous researches have used a fully developed turbulent flow condition of jet flow. In addition, the common way in numerical simulations for generating fully developed flow is by recycling, which do not accord to facts in experiments. Furthermore, limited research has been done on the influence of jet-to-co-flow velocity ratio. The researches of Antoine et al. [6], Gazzah et al. [7], and Djeridane [8] used different velocity ratios of 13.3, 5.7 and 10 in their work respectively; nonetheless, there is no research that integrating those different velocity ratios together to investigate their influence based on a fully developed jet condition.

In terms of particle-laden turbulent flow, most of the studies have focused on the effects of mass loading ratio Φ, the Stokes number Sk_0 on the particle behaviours of the particle-laden jets [9, 10]. However, less attention has been made to study the particle-laden co-flow jet. To be specific, limited research is carried out on the co-flow parameters, combined with their effect on both the carrier fluid and the dispersed particles, especially at a fully developed turbulence condition. In this paper, for a better understanding of the jet inflow that is employed in the design of a Solar Expanding-Vortex Receiver (SEVR), it is the aim of the present work to perform a fully developed turbulent jet flow at Re=10000, together with investigating the effects of velocity ratio on the characteristics of the jet and particles.

The present work is organized as follows. A single-phase turbulent flow in a straight pipe is performed based on LES method. This is followed by obtaining the adequate pipe length for achieving fully developed turbulent flow. A pipe flow with this determined pipe length is employed as the inflow of jet in the co-flow jet system, to generate a model of fully developed turbulent co-flow jet, which mimics a real jet generation. Three models with different velocity ratios (V_r =3, 6 and 12) are conducted for investigating the co-flow jet characteristics, including the decay of centreline velocity and turbulence intensities of the jet. Subsequently, particles are added under the one-way coupling and solved in a Lagrangian framework with varying the different velocity ratios of the particle-laden co-flow jet. Three models are simulated respectively for studying the distribution of particles.

Numerical approach

Simulation

In the present study, an open source CFD package, OpenFOAM (OpenCD Ltd.), was used to conduct the simulations. The Gauss linear corrected, Gauss self-filter central differencing and the Backward Euler are defined as the convection, diffusive and unsteady terms respectively. The velocity and pressure coupling field is solved by a standard PISO algorithm. The LES model with dynamic Smagorinsky procedure in sub-grid-scale [11, 12] is employed for turbulent pipe flow and jet simulation.

Single-phase pipe flow

A fully developed turbulent pipe flow is simulated in a straight pipe under an incompressible, isothermal condition. The computational domain length for the pipe is set to be long enough (L/D=200, where D is the pipe diameter), to ensure the pipe flow achieve fully developed stage. The bulk velocity of the pipe flow is denoted by U_b. The bulk Reynolds number is $Re_b=U_b\times D/\upsilon$=10000 (where υ is the dynamic viscosity), corresponding to a friction Reynolds number is Re_τ=295. For accelerating the process of reaching fully developed turbulence, an initial perturbation of 20% of the bulk velocity is introduced in the inlet flow. The layout of mesh of pipe is O-type, with the near wall grids being refined to resolve the turbulent boundary layer as presented in Figure 1. For the first near wall grid, Δy^+=0.94. The ratio of grid spacing to the Kolmogorov scale is 1.607. The sub-grid-scale part of the kinetic energy, i.e. the ratio

of k_{SGS}/k_{total} in the majority of the pipe flow is less than 0.2. The mesh is adequately resolved for LES simulation of pipe flow.

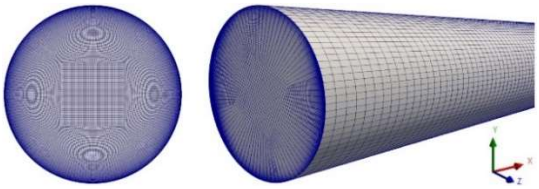

Figure 1. 3D view of the grid resolution of the straight pipe.

After one pipe length flow through, the streamwise mean velocity (U^+) profiles are obtained at different cross-sections located along the pipe (L/D=2, 4, 8, 16, 32 and 128). The convergence of those results is examined to determine the adequate pipe length for achieving fully developed stage.

Single-phase co-flow jet

Based on the fully developed single-phase pipe flow model, the desired length of the straight pipe is employed in the jet model to generate fully developed turbulent jet flow. The grid resolution and boundary conditions remain the same with pipe model. The computational domain of the jet model is shown in Figure 2 (a). The co-flow is performed by adding a large cylinder, with a sufficiently wide (20D) diameter. The velocity of co-flow is a uniform profile without any perturbation. The distance from jet nozzle to the outlet is 30D. The grids near the extended region of the pipe wall are refined to resolve the boundary layer of the jet, this is shown in Figure 2 (b) as below.

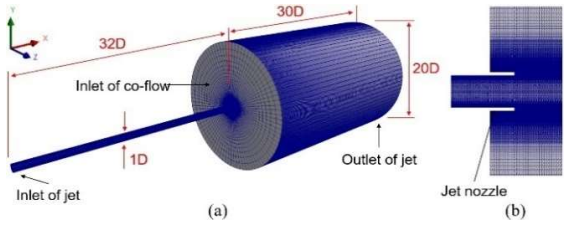

Figure 2. 3D view of the grid resolution of co-flow jet: (a) the overall view, (b) a part of the section plane.

The total number of grid points for the jet flow is approximately 9 million. Three different jet-to-co-flow velocity ratios (V_r=3, 6 and 12) are performed with the fixed bulk velocity U_b, to different co-flow velocities. After the flow has passed from the start of the jet to the outlet of the domain, the decay of streamwise velocity along the centreline, and the turbulence intensities at cross sections in downstream domain are extracted for postprocessing.

Particle-laden co-flow jet

Utilising one-way coupling for particles in the present work, only the Stokes drag force and gravity are considered that affect the translational motion of the individual particle. The passive particles are added on the flow fields via a Lagrangian framework. They are injected continuously from the inlet.

In present work, the Stokes number Sk_0 is defined as $Sk_0 = \frac{\rho_p d_p^2 U_b}{18\mu D} = 0.3$. The particle mass loading Φ_m is 3.31×10^{-3}, correspondingly, the volume fraction Φ_v is 0.6×10^{-6}, which is in the range of one-way coupling regime (Φ_v <10^{-6}). For the models with different velocity ratios, the particle distribution on the cross sections at different location of the domain (from the nozzle exit to outlet, x/D=0.2 to 30) are sampled.

Result and discussion

Pipe length for fully developed a turbulence

After temporal and spatial averaging of the velocity data at different locations along the pipe, the convergence of the mean streamwise velocity profiles is examined for finding the location that achieve fully developed stage. This is shown in Figure 3. The y axis represents the normalized mean streamwise velocity, $U^+=U_x/u_\tau$, where u_τ is the friction velocity, and the x axis is the inner scale $y^+=yu_\tau/\upsilon$, where the variable y is the wall-normal direction distance away from the wall. They are plotted in a logarithmic scale. The result of Figure 3 suggests that the mean streamwise velocities have not reached convergence before the location of L/D=32. After that location, the velocity profiles fit well with each other (three solid lines), which means the pipe flow has achieved fully developed stage after passing through L/D=32. The results show a high comparability with comparing to the DNS result of Chin et al. [13] as shown in the figure. This value of pipe length is chosen for the following jet models.

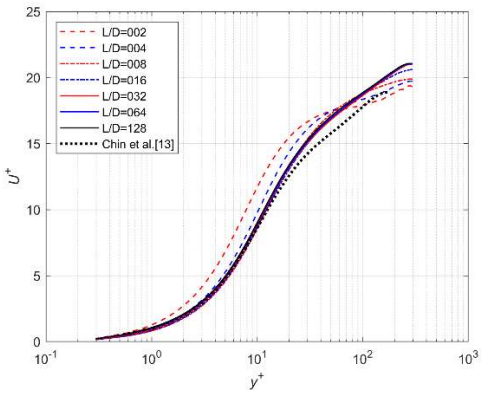

Figure 3. Mean streamwise velocity U^+ at different cross sections.

Instantaneous velocity fields of co-flow jet

Before viewing the mixing performance of co-flow jet, an instantaneous flow visualisation (Figure 4) of the co-flow jet mixing processes is obtained from the velocity fields. Figure 4 (a-c) show the comparison of models with the same boundary conditions but different velocity ratios (V_r=12, 6 and 3). All of them are illustrated in a same velocity range scale (0 to 1.25U_b).

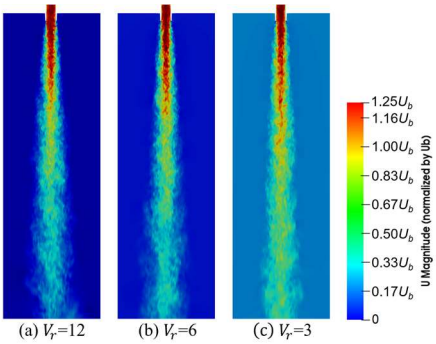

Figure 4. Instantaneous velocity fields of fully developed jets with different velocity ratios (a) V_r=12; (b) V_r=6; and (c) V_r=3.

It can be seen from Figure 4 that the high velocity of the jet (in red) is extended when the velocity ratio decreases. That means the model with smaller velocity ratio, i.e. a higher co-flow velocity, will slow down the decay of centreline velocities, along with slowing down the dissipation of velocities away from the centreline in the downstream domain.

The decay of axial velocities on centreline

The decays of the axial velocities on centreline of jet with different velocity ratios V_r, are shown in Figure 5. The x axis represents the normalized distance outside the nozzle exit along centreline, while the y axis represents the ratio of the centreline mean velocity excess at the jet nozzle exit (U_j) to the centreline mean velocity excess at the specific locations (U_c). It can be seen from Figure 5 that when V_r is decreased, i.e. a higher co-flow velocity, the jet will decay slower. This gives the interpretation for phenomenon on the downstream domain of the jet of the instantaneous velocity fields in Figure 4.

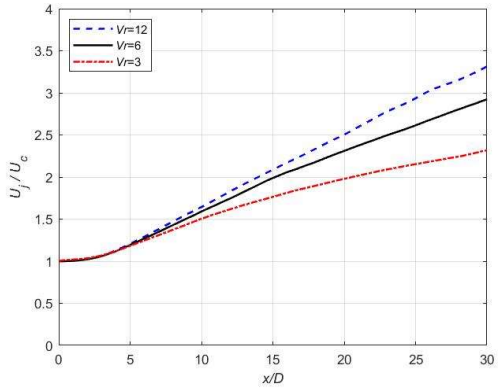

Figure 5. Decay of streamwise mean velocity on centreline.

Turbulence intensities

The turbulence intensities $u'u'$, $v'v'$ and $w'w'$ are plotted in Figure 6 (a-c) at different jet downstream locations, where u', v' and w' represent the fluctuating turbulent velocity components in the axial, radial and azimuthal directions respectively. The x axes represent the radial location that normalized by the downstream distance x-x_0, where x_0 is the axial distance from virtual origin to nozzle exit, which is about 1D. The y axes of all these turbulence intensities are normalized by ΔU_c, the difference between mean centreline velocity and local co-flow velocity. Also shown are the present results for a single jet, together with the previous experimental data of Panchapakesan & Lumley [2] and the DNS results of Picano & Casciola [3], presenting the same scale of turbulence intensities of a single jet without co-flow. Both previous data and present work are measured in a validated self-similar region of the jet, i.e. the profiles will not change much at different locations in the region. The x/D=25 is used in present work.

In Figure 6 (a), due to the max shear stress occurring when the jet spreading away from the centreline on the radial direction, there is a peak for the streamwise turbulence intensity. In present LES work of the single jet (V_r =infinity), this peak occurs at $r/(x\text{-}x_0)$≈0.053, which is slightly higher compared to 0.044 of the experiment of by Panchapakesan & Lumley [2] and 0.049 of the DNS results of Picano & Casciola [3]. Also, the peak value is lower than the published results. In terms of the radial and azimuthal turbulence intensities in Figure 6 (b) and (c), the present results of single jet are also slightly lower but showing a similar trend to the previous results. These deviations are mainly caused by different simulation methods, inflow conditions of the turbulence development and Reynolds numbers employed. Overall, the profiles of present result of single jet in Figure 6 show a well agreement with previous data.

For different velocity ratios, the value of turbulence intensities at the region of $r/(x\text{-}x_0)$<0.115 increases and the decay of turbulence intensities becomes faster at $r/(x\text{-}x_0)$>0.115 when the velocity ratio V_r decreases. The larger turbulence intensities are more distributed in the near jet axis region, while the turbulence intensities of the jet with larger V_r, are diffused faster when spreading far away from the jet axis.

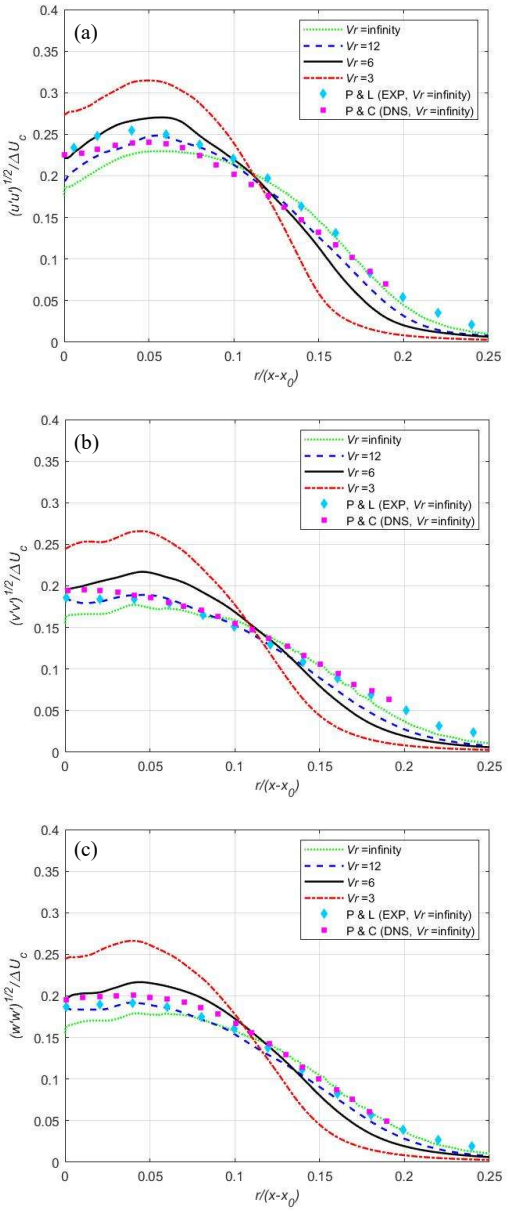

Figure 6. The (a) streamwise (b) radial and (c) azimuthal turbulence intensity profiles with different velocity ratios.

Particle distribution

To investigate the mechanisms leading to particle distribution difference in the jet domain, in Figure 7, we show the instantaneous distributions of particles on the section plane of the jet, with particles coloured by velocities. Figure 7 (a-c) show the velocity ratio of V_r =12, 6 and 3 respectively. The smaller co-flow velocity in Figure 7 (a) leads to the particles spreading more widely in the domain, while the larger co-flow velocity in Figure 7 (b) and (c) inhibits particles spreading. The particles are concentrated in the centre region. In other words, the particles of jet are spreading less with smaller V_r, which is consistent with the previous findings of the instantaneous velocity fields and turbulence intensities.

According to the locations shown in Figure 7 (c) in black dash lines, four cross sections at the locations of x/D=0.2, 10, 20 and 30 are extracted to acquire the particle distributions. The corres-

ponding results are shown in Figures 8, which illustrates the area-normalized probability of particle distributions *f(x)* against the diameter-normalized radial location.

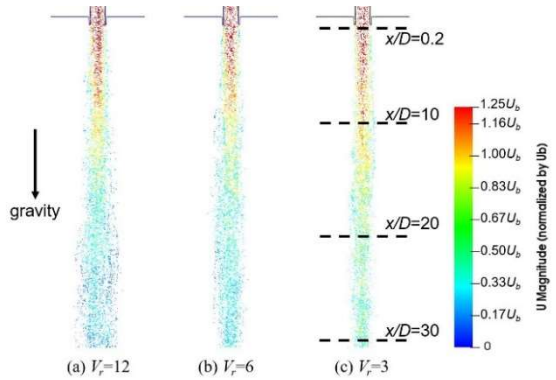

Figure 7. Instantaneous particle distribution of the particle-laden co-flow jets different velocity ratios of (a) V_r=12, (b) V_r=6 and (c) V_r=3.

As shown in Figure 8, the probability of particles distribution near the jet axis is increased with the decreasing of velocity ratio. Also, the probability outside away from the region in black dash lines (r/D<-0.5 & r/D>0.5) is decreased. These trends show a consistency with the change of turbulence intensities of different co-flow velocity jets in Figure 6.

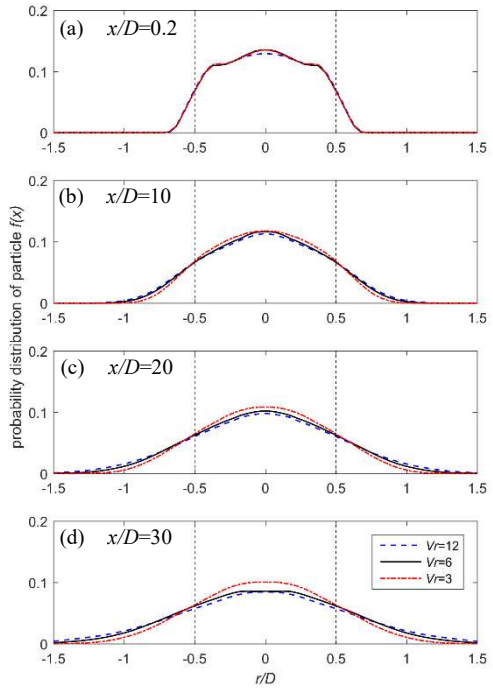

Figure 8. The probability of particle distribution with different velocity ratio at: (a) x/D=0.2, (b) x/D =10, (c) x/D =20, (d) x/D =30.

Conclusions

In this study, the inflow of the central jet is generated in a straight long pipe by means of LES method, with an adequate pipe length to achieve fully developed turbulence. The decay of streamwise centreline velocities of the co-flow jet has been calculated and indicated a slower trend of decay with the V_r decreasing from 12 to 3. The turbulence intensities of the co-flow jet have been calculated and compared with published results and show a well agreement. Also, the comparison of different velocity ratios has indicated a clear trend of increasing turbulence intensities in the centre region, and a trend of decreasing turbulence intensities in the shear layer with the V_r decreasing from 12 to 3. For the one-way coupling particle-laden jets, the effect of velocity ratio on particle distribution has indicated a similar trend with turbulence intensities, when the V_r decrease, the particles are more concentrated in the centre region, while more dispersed outside this region.

Acknowledgments

This work was supported with supercomputing resources provided by the Phoenix HPC service at the University of Adelaide. The authors would like to thank Professor Nathan and Dr Lau for the useful discussion on particle-laden jets. The authors acknowledge the financial support of the Australian Research Council.

References

[1] Abraham, J., Entrainment characteristics of transient gas jets. Numerical Heat Transfer Part A-Applications, 1996. 30(4): p. 347-364.

[2] Panchapakesan, N.R. and J.L. Lumley, Turbulence Measurements in Axisymmetrical Jets of Air and Helium .1. Air-Jet. Journal of Fluid Mechanics, 1993. 246: p. 197-223.

[3] Picano, F. and C.M. Casciola, Small-scale isotropy and universality of axisymmetric jets. Physics of Fluids, 2007. 19(11).

[4] Wang, P., et al., Large-eddy simulation of variable-density turbulent axisymmetric jets. International Journal of Heat and Fluid Flow, 2008. 29(3): p. 654-664.

[5] Srinivasarao, T., et al., Effect of Inner Nozzle Lip Thickness on Co-flow Jet Characteristics. International Journal of Turbo & Jet-Engines, 2017. 34(3): p. 287-293.

[6] Antoine, Y., F. Lemoine, and M. Lebouche, Turbulent transport of a passive scaler in a round jet discharging into a co-flowing stream. European Journal of Mechanics B-Fluids, 2001. 20(2): p. 275-301.

[7] Gazzah, M.H., et al., The dynamic field in turbulent round jet discharging into a co-flowing stream. Natural Science, 2010. 2(06): p. 635.

[8] Djeridane, T., Contribution à l'étude expérimentale de jets turbulents axisymétriques à densité variable. 1994, Université Aix-Marseille 2.

[9] Modarress, D., H. Tan, and S. Elghobashi, 2-Component Lda Measurement in a 2-Phase Turbulent Jet. Aiaa Journal, 1984. 22(5): p. 624-630.

[10] Lau, T.C.W. and G.J. Nathan, Influence of Stokes number on the velocity and concentration distributions in particle-laden jets. Journal of Fluid Mechanics, 2014. 757: p. 432-457.

[11] Germano, M., et al., *A Dynamic Subgrid-Scale Eddy Viscosity Model.* Physics of Fluids a-Fluid Dynamics, 1991. **3**(7): p. 1760-1765.

[12] Lilly, D.K., *A Proposed Modification of the Germano-Subgrid-Scale Closure Method.* Physics of Fluids a-Fluid Dynamics, 1992. **4**(3): p. 633-635.

[13] Chin, C., J. Monty, and A. Ooi, Reynolds number effects in DNS of pipe flow and comparison with channels and boundary layers. International Journal of Heat and Fluid Flow, 2014. 45: p. 33-40.